Filter and Processing Method to Improve R-Peak Detection for ECG Data with Motion Artefacts from Wearable Systems

Nadine R Lang[1*], Matthias Brischwein[1*], Erik Haßlmeyer[1*], Daniel Tantinger[1], Sven Feilner[1], Axel Heinrich[1], Heike Leutheuser[2], Stefan Gradl[2], Christian Weigand[1], Bjoern Eskofier [2], Matthias Struck[1]

[1]Fraunhofer Institute for Integrated Circuits IIS, Erlangen, Germany
[2]Digital Sports Group, Friedrich-Alexander University Erlangen-Nuremberg (FAU), Germany
*Authors contributed equally to this paper

Abstract

The electrocardiogram (ECG) is one of the most reliable information sources for assessing cardiovascular health and training success. Since the early 1990s, the heart rate variability (HRV), namely the variation from beat to beat, has become the focus of investigations as it provides insight into the complex interplay of body circulation and the influence of the autonomic nervous system on heartbeats. However, HRV parameters during physical activity are poorly understood, mostly due to the challenging signal processing in the presence of motion artefacts. To derive HRV parameters in time (heart rate (HR)) and frequency domains (high frequency (HF), low frequency (LF)), it is crucial to reliably detect the exact position of the R-peaks. We introduce a full algorithm chain where a sophisticated filtering technique is combined with an enhanced R-peak detection that can cope with motion artefacts in ECG data originating from physical activity.

1. Introduction

Since its development in the 19th century, the electrocardiogram of the heart (ECG) has been crucial to determine functions and failures of the heart. On the basis of modern ECG recordings it is possible to detect physical deformations of the heart (e.g. hypertrophy), as well as arrhythmia and extra systoles [1].

Recently, the interpretation of the heart rate variability (HRV), namely the temporal variation between individual beats of the heart, has become more and more interesting. For physiological interpretation, the exact detection of R-peaks and RR-intervals has become of crucial importance [2]. The subsequent transformation of RR-intervals into frequency domain reveals different frequency bands, known to be directly connected to the activation of the sympathetic and parasympathetic nervous system, thus the central nervous system [3].

Especially during physical activity, the ECG suffers from numerous motion artefacts, like random or stochastic noise leading to a distortion of the ECG and a significant reduction of the signal-to-noise ratio (SNR). Common ECG algorithms developed for clinical purposes are not designed for this purpose and therefore often show high false alarm rates, effectively causing misinterpretation of HRV parameters.

Various techniques have been proposed to cope with motion artefacts, in particular a set of filter techniques. Many algorithms use a high pass Finite Impulse Response (FIR) filter. Here, the output is taken after the FIR transfer is combined with a delay based on an integral number of the filter, offering a linear phase response and thus providing an undistorted ECG signal. However, the FIR filters needs a large number of filter coefficients to provide adequate signal characteristics, resulting in increased computational costs. Especially when it comes to mobile applications the requirement for low power consumption very much restricts the available computing resources and computational costs become increasingly important [4,5].

We suggest using a bidirectional Infinite Impulse Response (IIR) filter instead of a FIR filter. The recursive IIR filter offers a high quality output using fewer filter coefficients and therefore noticeable fewer computing time. The disadvantage of introducing a phase shift can be nullified by applying the filter bidirectional. To overcome the perturbing effects of motion artefacts, we introduce, subsequent to the filtering step, an R-peak detector based on a modified zero crossing algorithm to detect R-peaks. Here a set of possible R-peaks has to run through an additional plausibility routine which takes into account several temporal as well as morphological and contextual features to robustly decide whether the observed event belongs to a real R-peak or is an artifact. In this paper, we show that these enhancements can raise the detection rate of R-peaks in the special case of mobile recorded data. We compare our algorithm with the open source Hamilton algorithm [6].

2. Materials and methods

We compare our algorithm against the open source version of the Pan-Tompkins Algorithm as provided by Hamilton [7,6]. The Hamilton variant is developed to detect R-peaks from a clinical single-channel ECG device. The algorithm provides a positive predictive value of 96.48 % on the MIT/BIH arrhythmia database; however we use a self-assembled data base to be able to test the algorithms on data with motion artefacts.

2.1. Algorithm overview

The complete algorithm proposed in this paper consists of 4 stages. The raw signal is filtered with an analog band pass filter on the acquisition hardware. After the signal is digitized by an analog digital converter (ADC), it is filtered with a digital 50 Hz notch filter prior to a forward and backward IIR band pass filter (Fig. 1). Finally, the signal is further processed in the R-peak detection algorithm (Fig. 2).

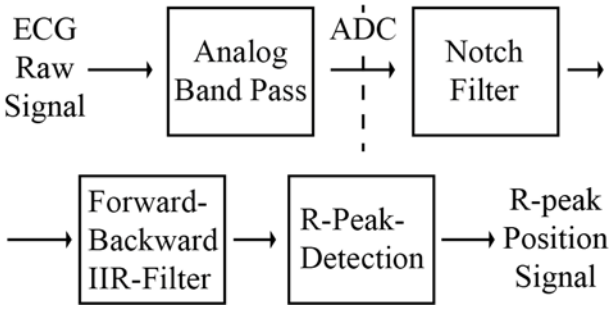

Figure 1: Algorithm Overview. The ECG raw signal is filtered with an analog band pass directly on the hardware. Afterwards, the signal is transformed into a digital signal by an ADC. After a digital band pass filter, the signal is filtered by an IIR filter in forward and backward direction, followed by the R-peak-detection.

Analog band pass filter: The frequency range of a normal ECG is traditionally defined between 0.67 Hz and 40 Hz. Due to the fact that we measure the ECG signal on a wearable system, we suffer from many artefacts like motion artefacts but also artefacts introduced by wires and electrostatic charge introduced by the textile components. To eliminate these mostly high frequent signals, the band pass filter has a range from 4 - 27 Hz and -10 dB.

Notch filter: To eliminate power line interference, we apply a 50 Hz Single Notch filter to compensate for electromagnetic irradiation.

IIR forward-backward filtering: After the raw signals are digitalized they are filtered with a three sections second order Butterworth IIR filter with cutoff frequencies of 8 Hz and 45 Hz at 3 dB.

Due to the nonlinear nature of the IIR filter a phase shift is introduced. To eliminate the phase shift, the window of n forward-filtered-samples is filtered in backwards direction with an IIR filter with the exact same filter coefficients as before. One advantage of an IIR filter over an FIR filter is the reduced number of filter coefficients which results in less operation per sample to reach comparable results.

R-peak detection: Subsequently to the filtering process QRS events are detected based on a zero-crossing QRS-detection algorithm suggested by Köhler et al. [8] and evaluated for mobile applications in Tantinger et al. [9]. In order to keep the sensitivity of the zero crossing detector under varying physical stress and therefore heart rates, we modified the algorithm by dynamically adjusting the parameter λ_Θ described as constant in [8] and which tunes the adaptivity i.e. the response time of the event thresholding to changing heart rates. The threshold adaptivity is in our case updated according to

$$\lambda_\Theta = h_{max} - \frac{\lambda_{\Theta,max} - \lambda_{\Theta,min}}{h_{max} - h_{min}} (h(t) - h_{min}),$$

where $h(t)$ ($h \in [h_{min}; h_{max}]$) is the heart rate at time t in beats per minute (bpm) and $\lambda_\Theta \in [\lambda_{\Theta,min}; \lambda_{\Theta,max}]$. To cope with the low SNR we further extend the algorithm with an additional processing step which tracks the history of R-peaks over time to increase the reliability of the detection. Basically, this filter is an adaptive prediction-correction filter which iteratively transforms a set of R-peak candidates into a new set of robust R-peaks, based on an average model of an R-peak (Fig.2). The algorithm works as follows:

Input is a set of R-peak candidates from the zero crossing step and a prediction about the next R-peak location which is estimated by means of a lower and an upper bound for the next regular R-peak. The set of candidate R-peaks is labeled into subsets of early systoles, regular systoles and far systoles, based on the prediction of the next R-peak. If there are extrasystoles, the best match within the respective set is accepted as robust R-peak. As best match we define the candidate with highest R-peak response. If there are no extra systoles found, the best match within the set of regular systoles is selected. Given there are only far systoles found, the best match within this class is accepted only if no regular systole was missed by the zero-crossing R-peak detector. To ensure this, another maximum-minimum search for a potentially missed regular R-peak is performed on the backward filtered signal within the expected time frame. Given that another R-peak candidate is found, and accepted by the classifier, this candidate is preferred to the far systole as new robust R-peak.

Whenever an R-peak is accepted to the set of robust peaks, all candidates found prior to the accepted one are discarded. No R-peak candidates following the accepted R-peak are lost. The model is updated and a new iteration

in the process described above is performed until the set of candidates runs empty or the cumulative RR-interval time of candidates falls below the predicted upper bound RR interval.

Further note that the remaining candidates may be classified differently in the next iteration because the prediction as well as the model is updated with every accepted R-peak. To bootstrap our algorithm, the first ten R-peak candidates are accepted without verification against model and prediction. As R-peak we consider a feature vector $\vec{x}$ which is extracted from the backward filtered ECG signal within the QRS event frame received from the zero crossing detector (Fig. 2).

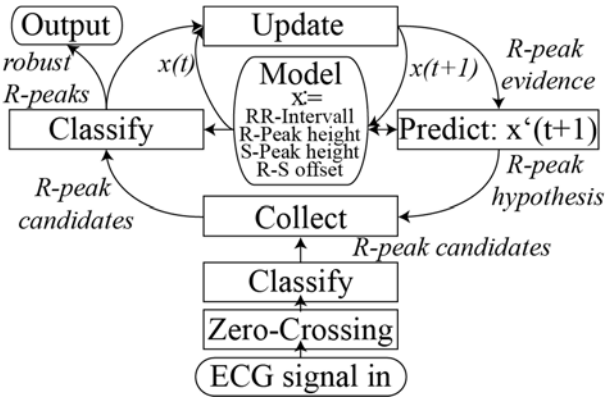

Figure 2: R-peak-algorithm overview. The filtered ECG signal is handed over to the Zero-Crossing step, where a first classification is performed. Next, the number of R-peak candidates is collected and further classified by comparison with a given model. Robust R-peaks are subsequently used to update the model. Rectangular boxes resemble states of processing, while rounded boxes are signals. Arrows visualize data flow.

2.2. FitnessSHIRT

Mobile ECG data is recorded with the Fraunhofer IIS FitnessSHIRT. Two textile ECG sensors are integrated in the shirt on both sides of the thorax in order to derive a single-channel ECG. The data is acquired at a sampling rate of 1024 Hz. Long-time data acquisition is realized on a microSD card, connected to the main module and attached to the shirt. An integrated Bluetooth module allows transmitting the raw data to a portable device (smartphone or tablet) or a PC for real-time visualization and post-processing.

2.3. Test protocol and data base

All persons were provided with a well-fitting FitnessSHIRT. The test protocol is adapted from a Bruce test. The test persons had to perform 2 exercises. The running exercise consisted of a 5 minute running phase at 10 km/h followed by an increase of 1 km/h every 3 minutes until test persons feel exhausted. The ergometer exercise began at 130 W load followed by an increase of 30 W every 3 minutes until test persons feel exhausted. Care was taken that 65-70 rpm was kept constantly.

All persons were healthy males of average fitness level and average age of 31.6 years. We analyzed running data from 10 persons and ergometer data from 25 persons. ECG data were manually annotated.

3. Results and discussion

As a measure of comparison, we evaluate the True Positive Rate (TPR) and the Positive Predictive Value (PPV), defined as

$$TPR = TP \,/\, (TP + FN)$$
$$PPV = TP \,/\, (TP + FP)$$

with

TP: True Positive total number of correct detections,
FP: False Positive total number of false detections,
FN: False Negative total number of missed detections.

As a consequence of phase delays introduced with the filtering, detected R-peaks often do not exactly match the annotation. Therefore, we choose an acceptance radius around each annotation and employ nearest neighbor search prior to distance thresholding to match annotations to detections and to decide for each of above cases. Comparing 20 sets of data with about 8193 hand annotated R-peaks, we find that our algorithm has a TPR of 90.0 % (on ergometer data), when the acceptance radius is chosen for three samples, corresponding to an accuracy of 6 ms. The Hamilton algorithm has in this case only a TPR of 62.2 %. If we increase the tolerance radius, the PPV of both algorithms raises (Tab. 1).
Our algorithm reaches a TPR of over 99 % for an acceptance radius bigger than 8 whereas the Hamilton algorithm reaches comparable detection rates earliest at a radius of 15, corresponding to ~30 ms. This shows that our algorithm performs almost twice as accurate as Hamilton's algorithm under the conditions mentioned.
Note, that the algorithm in [7] was established to find the position of QRS complexes, not necessarily R-peaks. If the aim is however, to derive HRV features, the exact R-peak position has to be known. Moreover, the Hamilton was developed to evaluate clinical ECG signal whereas we use mobile recorded data with motion artefacts.

4. Conclusion

We conclude that our R-peak detection algorithm outperforms the reference method in situations when ECG signals are superimposed with motion artifacts. However, further optimizations might be necessary when activity data is not measured in laboratory conditions.

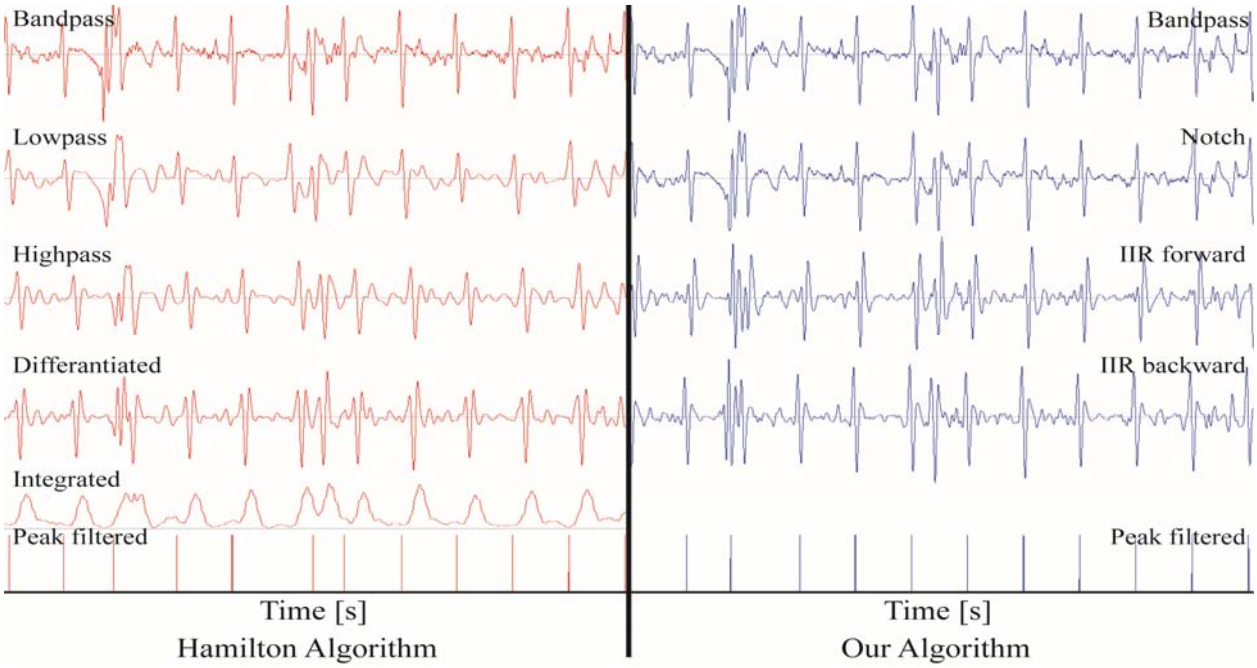

Figure 3: Processing steps as performed by Hamilton (left) and our algorithm (right) on a segment record over 4 seconds of training activity. Both algorithms perform multiple filtering steps before R-peaks are detected. When the signals are forged by motion artefacts (e.g. at ~2 s), the proposed algorithm still reliably detects the R-peaks, demonstrating the robustness of our method. Note that ECG signals were band pass filtered on the hardware.

	TPR ($r = 3$) running	TPR ($r = 3$) ergometer	TPR ($r = 8$) running	TPR ($r = 8$) ergometer
Hamilton	25.3%	62.2%	65.7%	86.1%
Ours	84.6%	90.0%	98.2%	99.2%

	PPV ($r = 3$) running	PPV ($r = 3$) ergometer	PPV ($r = 8$) running	PPV ($r = 8$) ergometer
Hamilton	23.9%	60.7%	63.3%	84.5%
Ours	81.2%	88.0%	95.2%	97.2%

Table 1: True positive rate (TPR) and Positive Predictive Value (PPV) of our algorithm compared to Hamilton. We tested with different acceptance radii (r in samples) and distinguished between running experiments and ergometer experiments. In all cases our algorithm outperforms the reference method.

Acknowledgements

This contribution was supported by the Bavarian Ministry of Economic Affairs and Media, Energy and Technology as a part of the Bavarian project ”Leistungszentrum Elektroniksysteme (LZE)”

References

[1] Alfakih K, Walters K, Jones T, Ridgway J, Hall AS, Sivananthan M. New Gender-Specific Partition Values for ECG Criteria of Left Ventricular Hypertrophy: Recalibration Against Cardiac MRI. Hypertension. 2004 Aug 1;44(2):175–9.

[2] Elgendi M, Eskofier B, Abbott D. Fast T Wave Detection Calibrated by Clinical Knowledge with Annotation of P and T Waves. Sensors. 2015 Jul 21;15(7):17693–714.

[3] Malik M. Heart rate variability. Ann Noninvasive Electrocardiol. 1996;1(2):151–81.

[4] Tobola A, Espig C, Streit FJ, Korpok O, Schmitz B, Hofmann C, et al. Scalable ECG hardware and algorithms for extended runtime of wearable sensors. Medical Measurements and Applications (MeMeA), 2015 IEEE International Symposium. p. 255–60. 209

[5] Elgendi M, Eskofier B, Dokos S, Abbott D. Revisiting QRS Detection Methodologies for Portable, Wearable, Battery-Operated, and Wireless ECG Systems. Amaral LAN, editor. PLoS ONE. 2014 Jan 7;9(1):e84018.

[6] Hamilton P. Open source ECG analysis. In: Computers in Cardiology IEEE; 2002 p. 101–4.

[7] Pan J, Tompkins WJ. A real-time QRS detection algorithm. Biomed Eng IEEE Trans On. 1985;(3):230–6.

[8] Kohler BU, Hennig C, Orglmeister R. QRS detection using zero crossing counts. Appl Genomics Proteomics. 2003;2(2):138–45.

[9] Tantinger D, Feilner S, Schmitz D, Weigand C, Hofmann C, Struck M. Evaluation of QRS detection algorithm implemented for mobile applications based on ECG data acquired from sensorized garments. Biomed Eng Biomed Tech [Internet]. 2012

Address for correspondence:
Nadine Lang, nadine.lang@iis.fraunhofer.de